

## ESTIMATION OF DISCRETIZATION ERROR IN TIME AND SPACE DOMAIN OF NUMERICAL HEAT CONDUCTION

M. Pohanka\*

***Summary:** The numerical approach requires some simplification of continuous physical systems. The simplification is used for the object, its boundary conditions, and the time domain. The approach that uses stress energy in mechanics can analogically be applied to the finite difference method of the unsteady heat conduction with temperature dependent material properties where the boundary conditions are assumed to be constant within one time step. Estimation of discretization error of the boundary conditions in the time domain, and of mesh discretization error in both the space and time domain is described in the paper. Some numerical tests are presented and method for discretization optimization is proposed.*

### 1. Introduction

Efficient, accurate and stable numerical methods for solving heat transfer processes are of great importance in many industrial applications. It is nowadays generally recognized that computer analysis of complex problems may provide a cost-effective, quick and sufficiently reliable method in many cases. Sometimes, the computational methods may also be an alternative or a complement to experimental investigations.

Although computation of heat transfer has reached a certain level and it can be significantly helpful in many engineering and industrial applications, still a comprehensive research is needed in, e.g., heat transfer, handling of complex geometries, etc. Performing various heat transfer experimental analyses, a very important problem arises: How precise are the computed data? An answer to this question has a much wider range of applicability than it could seem. The knowledge of precision of the computed results can be very useful for uncovering the weakest points in performing a complicated and interconnected heat transfer experimental analysis. During the analysis, an experiment and a computational part are performed. In both the experiment and the computational part, a number of various errors are accumulated, such as activation error, error in measured data, assumption error, error due to the computational model simplification, and various numerical errors (iterations, rounding, etc.).

Adaptively generated models are very efficient, but so far only a few papers dealing with the unsteady heat conduction problem have been published. In addition, the precision of the computed results is hardly known. These problems increase for experiments with rapid changes in boundary conditions.

---

\* Ing. Michal Pohanka: Heat Transfer and Fluid Flow Laboratory; Brno University of Technology; Faculty of Mechanical Engineering; Technická 2896/2; 616 69 Brno; Czech Republic; Phone +420 54114 3283; Fax +420 54114 2224; E-mail: pohanka@fme.vutbr.cz

In this paper, attention is focused on the estimation of errors of the computed results to increase the precision of the computed results. For complex geometries, there are no exact analytical solutions and thus numerical methods must be used. The numerical methods simplify the reality – e.g. the temperature profile is piecewise linearized. This simplification leads to a computational error which increases for highly transient problems. A method for an adaptively generated mesh of the computational model on the basis of the estimated error is suggested. During computation, time dependent boundary conditions are also simplified. An automatic time-step refinement for unsteady problems is also important to achieve the desired accuracy.

## 2. Discretization Error Estimation

The numerical approach requires some simplification of continuous physical systems. The simplification is used for the object, its boundary conditions, and the time domain. The approach that uses stress energy in mechanics can analogically be applied to heat conduction. The heat energy is used for an accuracy analysis of heat conduction problems solved using the numerical approach instead of stress energy.

### Heat Conduction Equations

For unsteady one-dimensional (1D) heat conduction in Cartesian coordinates, the general form of the *heat diffusion equation* (Incropera, 1996) also known as the *heat equation*, can be written as

$$\frac{dq}{dx} + \dot{q} = \rho \cdot c \frac{dT}{dt} \quad (1)$$

where

$$q = k \frac{dT}{dx} . \quad (2)$$

The time domain is discretized into the time steps where the index of the current time step is  $m$  and the time step is defined as

$$\Delta t = t^m - t^{m-1} \approx dt . \quad (3)$$

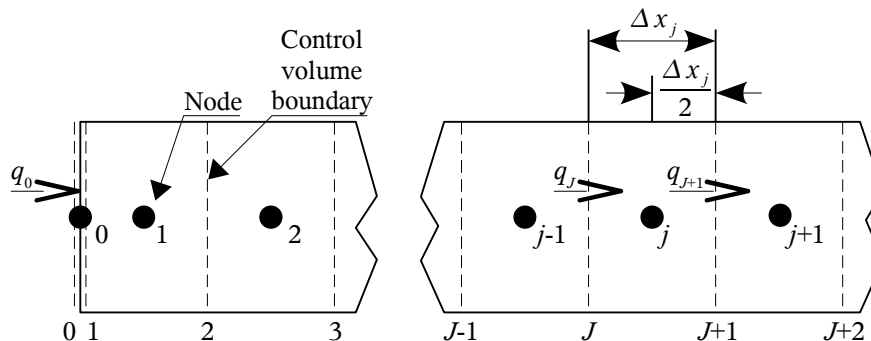


Figure 1 – One-dimensional model for planar geometry showing control volume and its boundaries.

The object domain is discretized into a number of control volumes (see Figure 1). Some methods suggest to create the surface volume of zero thickness and others suggest the use of the surface volume of half size of the interior volumes. We use zero thickness, because we do not use the constant size of the interior volumes. This enables us to create a small volume next to the zero-volume which gives us the possibility to compute the surface temperature more accurately.

For each control volume, conservation of energy is applied to derive a set of algebraic equations (Patankar, 1980). Integrating Eq. (1) over the  $j$ -th control volume, we can write

$$q_J^m - q_{J+1}^m + \Delta x_j \cdot \dot{q}_j = \Delta x_j \cdot \rho_j(T_j^m) \cdot c_j(T_j^m) \cdot \frac{T_j^m - T_j^{m-1}}{\Delta t} \quad (4)$$

where  $\rho_j(T_j^m)$  and  $c_j(T_j^m)$  are the temperature-dependent mass density and specific heat, respectively,  $T_j^{m-1}$  is the temperature of the node in the previous time step and  $\Delta t$  is the time step. When the mass density  $\rho$  or specific heat  $c$  becomes more dependent on the temperature (e.g. a phase change), the results are more inaccurate. This problem can be eliminated by solving the equations using the enthalpy instead of specific heat and mass density as described by Pohanka, (2003).

Because the conductivities  $k_{j-1}$  and  $k_j$  of the neighboring volumes may be different, there may be a discontinuity of the slope ( $dT/dx$ ) at the control-volume boundary. The heat flux  $q_J^m$  of Eq. (4) can be evaluated on the  $J$ -th boundary at the time step  $m$  as

$$q_J^m = \left[ \frac{\frac{\Delta x_{j-1}}{2}}{k_{j-1}(T_{j-1}^m)} + \frac{\frac{\Delta x_j}{2}}{k_j(T_j^m)} \right]^{-1} \cdot (T_{j-1}^m - T_j^m) \quad (5)$$

where  $j$  is the node index,  $k_j(T_j^m)$  is temperature-dependent thermal conductivity, and the  $m$  superscript represents the time index.

### Boundary Conditions

We are working with unsteady boundary conditions but the boundary conditions are assumed to be constant within one time step as can be seen from Eqs. (4) and (5). Therefore, the time dependent profile of boundary conditions must be replaced by a discontinuous profile consisting of a number of small constant pieces. Their length is the time step (see Figure 2).

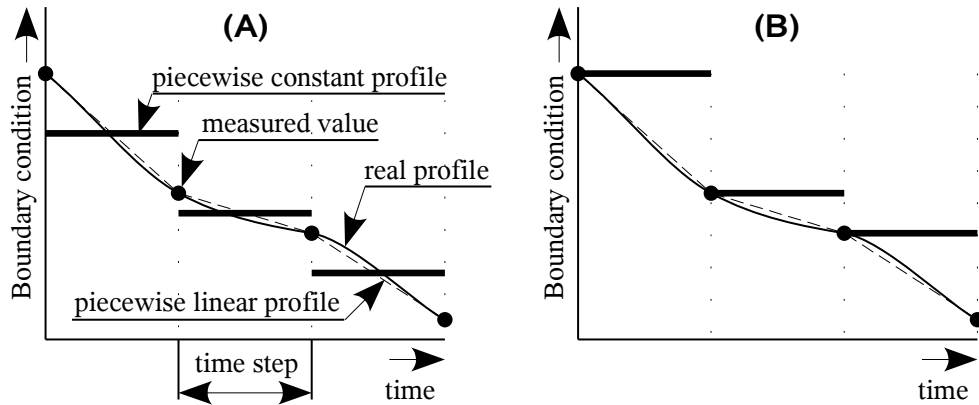


Figure 2 – Simplification of time-dependent boundary conditions.

In most cases we do not know the real profile of boundary conditions, we only know the values in certain measured time instants (see Figure 2). We usually use a piecewise linearized profile between the measured values. Knowing the boundary conditions in certain measured time instants, we can simplify them in various ways. Two methods are shown in Figure 3. Method **B** is often used, but method **A** is more effective.

We can estimate the error of simplified boundary conditions for case **A** as a sum of partial errors

$$\xi_x = \sum_{m=1}^n \left| \frac{\tilde{\chi}_m - \tilde{\chi}_{m-1}}{4} \right| \quad (6)$$

where  $\tilde{\chi}_m$  is the measured boundary condition at time step  $m$  and  $n$  is the number of computed time steps. The estimated error for case **B** is twice higher.

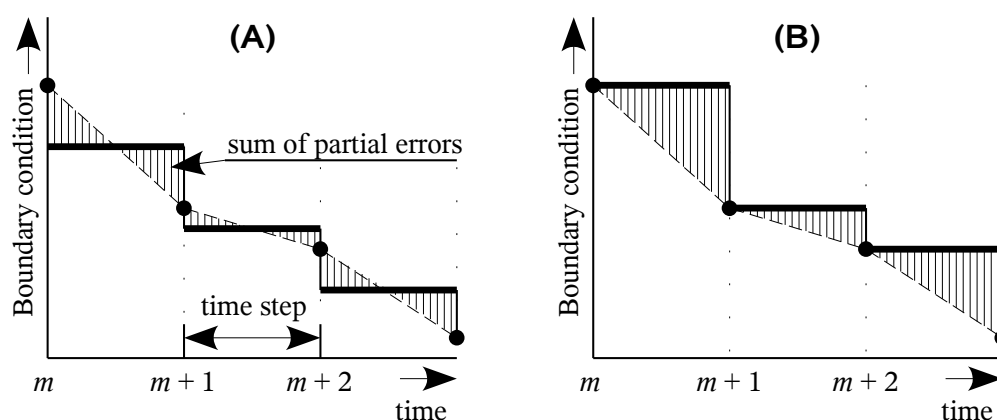


Figure 3 – Boundary conditions error estimation.

#### Mesh Discretization Error

For rapid changes in the heat flux boundary conditions and near the heterogeneous material, a fine mesh is required. This is because the smooth temperature profile has been piecewise linearized. Figure 4 shows two meshes – a rough one and a finer one. Before any estimation of the mesh discretization error and any mesh refinement can be done, the user must create a fine mesh that reflects the expected temperature profile. If the user creates a rough mesh (case **A**), the analysis skips the left temperature peak. If the mesh is fine enough (case **B**), the mesh discretization error can be computed, and based on this information the mesh refinement can be done.

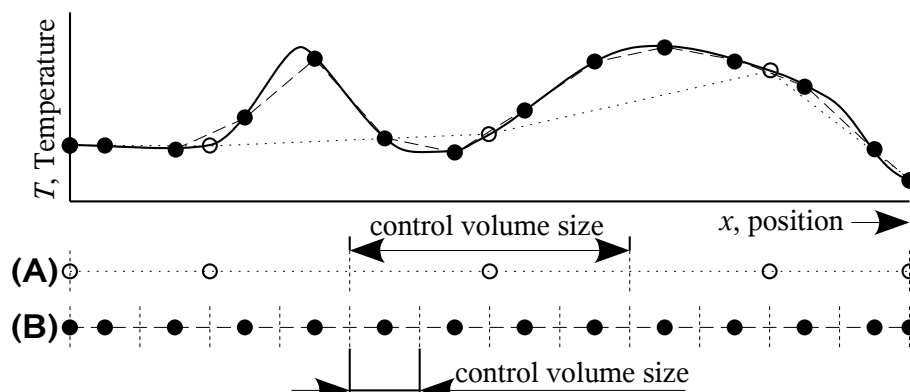


Figure 4 – Mesh design.

We investigate the mesh discretization error by comparing the heat energy stored within the control volume. The heat energy of the control volume can be expressed as an enthalpy

$$H_j^* = \frac{1}{\Delta x_j} \int_{x=x_j}^{x_{j+1}} \int_{T_{ref}}^T \rho \cdot c \, dT \, dx. \quad (7)$$

Because we are assuming constant material properties within one control volume, we can simplify Eq. (7) as follows

$$H_j^* = \rho \cdot c \cdot \bar{T}_j^*. \quad (8)$$

This simplifies our search for the mesh discretization error. We can only investigate the average temperature of the control volume and, if necessary, we can recalculate the average temperature to heat energy using Eq. (8). We can assume two extreme conditions shown in Figure 5. Case **A** shows the situation shortly after the rise in temperature of the control volume  $j - 1$ . The temperature on the boundary  $T_j$  is very high compared to the rest of the temperatures within the control volume  $j$ . Case **B** shows the situation later after the change. The thermal shock propagates deeper inside the control volume. Because of the piecewise linearized profile, we only know the temperature at the center of the node and we can estimate the temperature on its boundaries. We do not know anything about the real temperature profile between the centers of the control volumes. However, we can express the two extreme conditions shown in Figure 5. As you can see in case **A**, the real average temperature of the  $j^{\text{th}}$  control volume  $\bar{T}_j^*$  is very close to the temperature of the  $j^{\text{th}}$  node  $T_j$ . On the other hand, in case **B**, the real average temperature is much closer to the average temperature computed from the temperatures of the node and on the boundaries of the control volume as follows

$$\bar{T}_j = \frac{\bar{T}_{j,j} + \bar{T}_{j,j+1}}{2} = \frac{(T_j + T_j)/2 + (T_j + T_{j+1})/2}{2}. \quad (9)$$

If we take a closer look at FDM and FVM, we find that the FDM assumes the temperature of the node  $T_j$  for the average temperature of the control volume, while the FVM assumes  $\bar{T}_j$  expressed in Eq. (9).

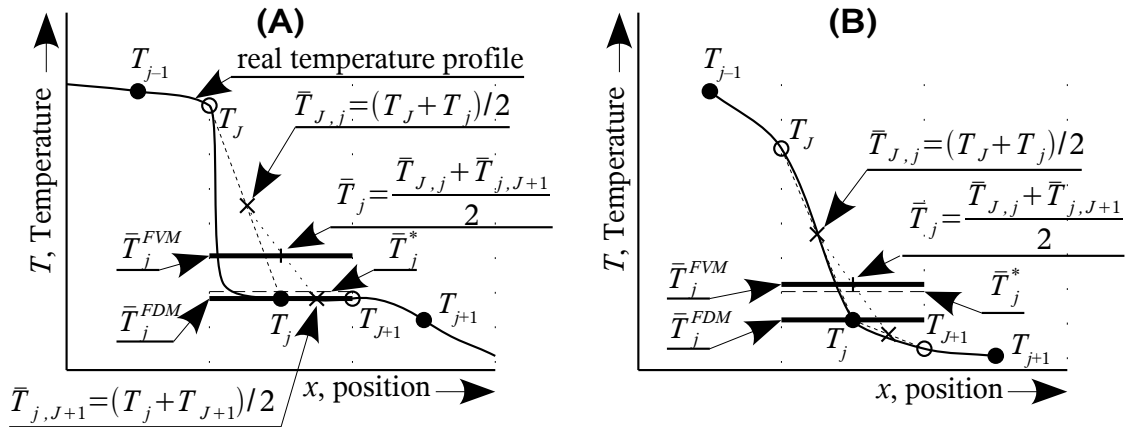


Figure 5 – Temperature of a control volume in FDM, FVM, and real average temperature of the control volume.

Assuming the real average temperature is between the  $\bar{T}_j^{FDM}$  and  $\bar{T}_j^{FVM}$ , we can estimate the discretization error as the difference between the temperature at the center of the node and the average temperature  $\bar{T}_j$  using Eq. (9) as follows:

$$\xi_{\bar{T}} = \bar{T}_j^{FDM} - \bar{T}_j^{FVM} = T_j - \bar{T}_j = \frac{T_j}{2} - \frac{1}{4} \frac{k_{j-1}(T_{j-1}) \cdot \Delta x_j \cdot T_{j-1} + k_j(T_j) \cdot \Delta x_{j-1} \cdot T_j}{k_{j-1}(T_{j-1}) \cdot \Delta x_j + k_j(T_j) \cdot \Delta x_{j-1}} - \frac{1}{4} \frac{k_j(T_j) \cdot \Delta x_{j+1} \cdot T_j + k_{j+1}(T_{j+1}) \cdot \Delta x_j \cdot T_{j+1}}{k_j(T_j) \cdot \Delta x_{j+1} + k_{j+1}(T_{j+1}) \cdot \Delta x_j} \quad (10)$$

The same equation can be obtained for cylindrical coordinates. Only  $x$  is replaced by  $r$ .

#### Time Discretization Error

Dealing with time discretization, we should compare the three main schemes for temperature variation in time – an explicit, Crank-Nicholson, and fully implicit one. The explicit scheme essentially assumes that the old temperature lasts through the entire time step. The fully implicit scheme supposes that the temperature suddenly drops at the beginning of the time step and stays over the whole time step, while the Crank-Nicholson scheme assumes a linear variation of the temperature during the time step. Working only with the unconditionally stable fully implicit scheme, we derive a method for estimating the error caused by time discretization. As you can see in Figure 6, none method describes correctly the variation of temperature in time shortly after a change in the boundary condition.

The trick to estimate the error caused by time discretization is based on comparing the error of the temperature (hatched area in Figure 6) for the time step and the double time step. As you can see, for the later change in boundary condition, the hatched area for the double time step is about twice larger than that for two steps of the normal time step. Knowing that the error (the hatched area) is half the size of that for the half time step and having computed our problem under solution using the double time step and normal time step we can estimate the error caused by time discretization as

$$\xi_{\Delta t}(T_j) = |T_j'' - T_j'| \quad (11)$$

where  $T_j''$  is the temperature computed using the double time step and  $T_j'$  is the temperature computed using the normal time step.

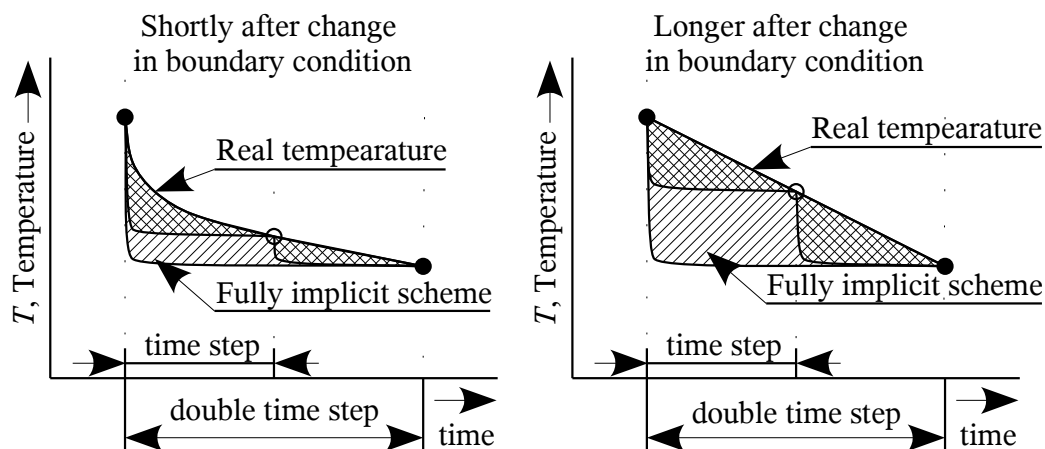


Figure 6 – Temperature variation and time step refinement.

The situation is slightly different for the case shortly after the change in boundary condition, because the hatched area for the double time step is not twice larger than that for two steps of the normal time step, but slightly less. No ratio lower than 1.5 was observed when testing the method; the lowest values did not drop under 1.7. Knowing this behavior and applying this ratio in the equation describing the sum of a geometric series, we can estimate the error caused by time discretization as

$$\xi_{\Delta t}(T_j) = \kappa \cdot |T_j'' - T_j'| \quad (12)$$

where the  $\kappa$  coefficient varies from 1 to 2, depending on the problem under solution. The  $\kappa=2$  should be used to make sure that the estimation of the maximum error caused by time discretization is correct ( $\kappa=2$  for ratio 1.5 and  $\kappa=1$  for ratio 2). For the infinite time step (steady conditions), the implicit scheme describes the temperature variation in time almost perfectly and there is no need to make such an estimation.

### 3. Optimization of Discretization

Knowing the methods for discretization error estimation, we can use them for mesh and time step optimization. The next sections describe the methods for setting the optimal mesh and time steps, but first we deal with refinement of boundary conditions measured in discrete time instants.

#### *Refinement of Boundary Conditions in Time Domain*

Before mesh optimization can be done, appropriate boundary conditions should be prepared. We assume boundary conditions measured in discrete time instants and the linearized profile between the measured values. However, the computation numerical method assumes constant boundary conditions within one time step. Figure 7 shows that the error is half the size of that for a half time step. This behavior can be used for time step refinement. Error caused by simplification can be expressed as

$$\Delta t = \frac{\Delta t^*}{\text{trunc}\left(\xi_x^* / \xi_x^{\max} + 1\right)} \quad (13)$$

where  $\Delta t$  is a new time step,  $\Delta t^*$  is time discretization of measured boundary condition,  $\xi_x^*$  is the sum of the partial error for the time step  $\Delta t^*$ ,  $\xi_x^{\max}$  is the maximum allowed value, and the *trunc* function returns only the integer part of the expression in brackets.

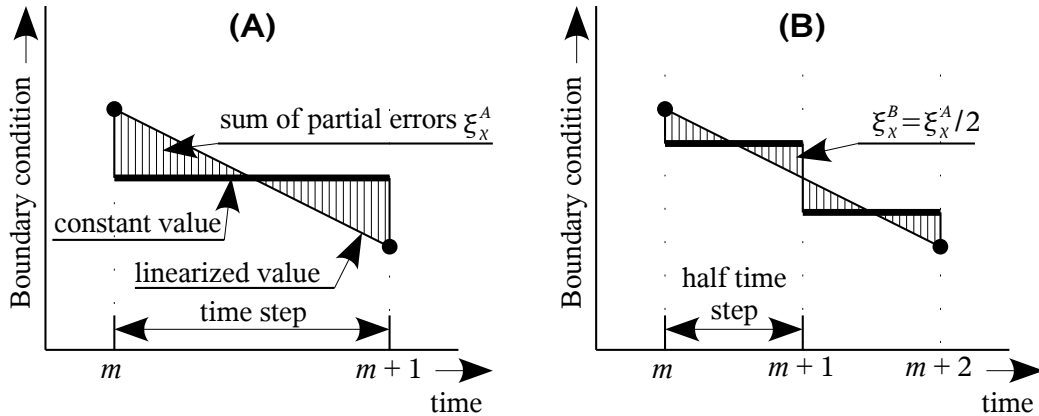


Figure 7 – Boundary condition refinement.

### *Mesh Optimization*

In the forward solver, an adaptive meshing scheme should be used to keep the number of computational points at minimum whilst ensuring accuracy of the solution. The linearized profile will give reasonable representation of the solution only if the grid is sufficiently fine. Before mesh optimization can be done, a starting one must be created. The starting mesh should not be very rough (see Figure 4). The mesh must reflect the expected temperature profile. It is better to create a finer mesh, which can be coarsened, than to create a too rough one.

Eq. (10) is used as a criterion equation for mesh refinement. If the  $\xi_{\bar{T}}$  parameter is higher than our acceptable value  $\xi_{\bar{T}}^{max}$ , the control volume should be divided into more control volumes. If the center node of a control volume corresponds to a temperature sensor location, the volume should be divided into an odd number of volumes so that the position of the center node remains unchanged. If the  $\xi_{\bar{T}}$  parameter is lower for two neighboring control volumes than the limit value  $\xi_{\bar{T}}^{min}$ , the control volumes can be merged. However, avoid merging volumes corresponding to a temperature sensor location and volumes already divided. The  $\xi_{\bar{T}}$  parameters should be checked for all control volumes after each time step and the computation along with mesh refinement should be repeated until no re-meshing is necessary.

### *Time Step Refinement*

The used fully implicit scheme does not precisely describe the temperature variation of control volumes in time, which causes some inaccuracy. As shown in Figure 6, the finer time step results in a higher accuracy of the computed result. The estimated error caused by time discretization is expressed by Eq. (12). This error should be checked after computation. If the error is higher than the acceptable value  $\xi_{\Delta t}^{max}$ , the problem should be computed using the half time step. This approach allows us to use repeatedly Eq. (12).

## **4. Results – Verification of Discretization Error Estimation**

### *Boundary Conditions and Time Discretization Error*

To verify the method for estimation of time discretization error using Eq. (12) a one-dimensional model was used. The model was assumed to be made of stainless steel. The length of the model was 10 mm for all tests except the one with a constant heat transfer coefficient where the length was 100 mm. One side of the model was insulated while the other one was exposed to various boundary conditions. Starting temperature of the model was 0°C.

First, a single and two time steps were tested. A constant heat flux of 100 000 W/m<sup>2</sup> was applied to one boundary. The duration was 1 s and 10 s for the first and second experiment, respectively. The computed temperature profiles using a very fine time step are represented in Figures 8–9 by the solid line with crosses. These temperature profiles were compared with those computed using a single time step of duration of 1 s and 10 s for the first and second experiment, respectively. The computed differences are represented in Figures 8–9 by the thick solid black line. To verify Eq. (12) for estimation of time discretization error, temperature profiles were also computed using half time steps. The estimated errors were computed for  $\kappa=1; 1.5; 2$  and are shown in Figures 8–9. It is obvious that the estimated errors computed using  $\kappa=2$  and 1.5 well cover the error caused by the time discretization for the half time step. The only place where the error is bigger than the estimated one is where



the error is very low. However, in most cases the important value is the maximum error that is correctly determined.

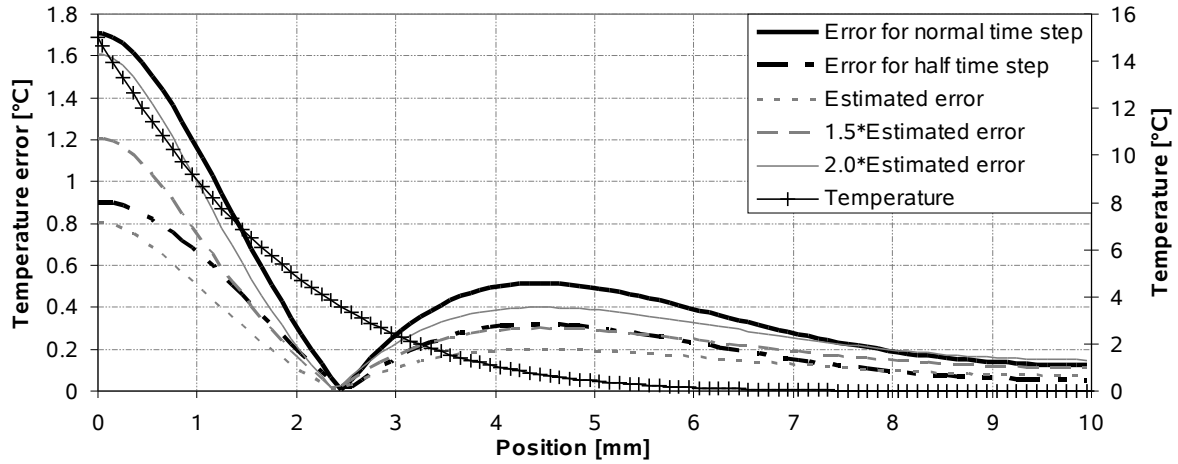


Figure 8 – Temperature profile for a constant heat flux of 100 000 W/m<sup>2</sup> after 1 s.

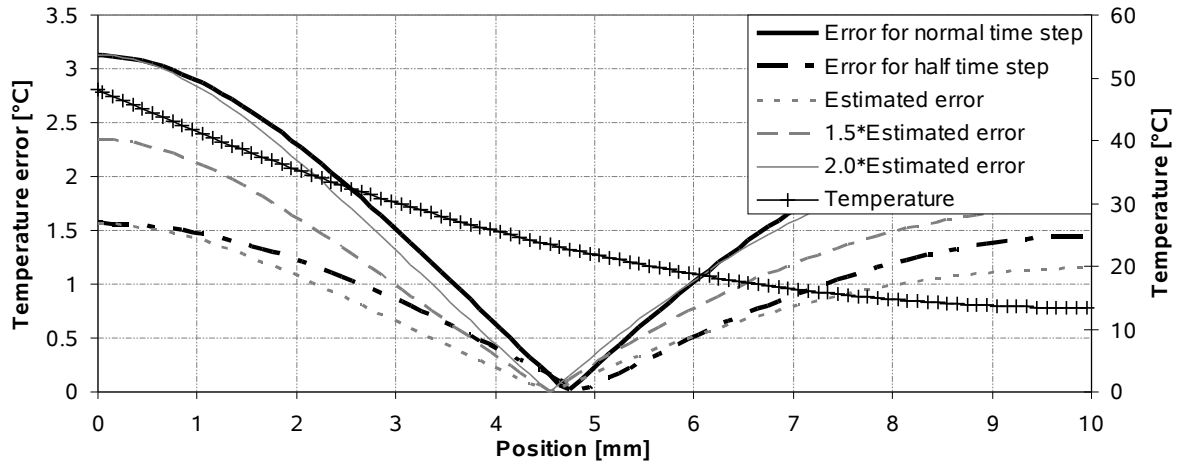


Figure 9 – Temperature profile for a constant heat flux of 100 000 W/m<sup>2</sup>.K after 10 s.

The estimation algorithm was also verified for time dependent boundary conditions. The sinusoid heat flux and constant heat transfer coefficient were used as shown in Figures 10 and 12. The charts show real boundary conditions and discretized ones for time normal and half time steps. The computed temperature profiles, time discretization errors, and estimated errors are shown in Figures 11 and 13. It is obvious that the estimated errors computed using  $\kappa=2$  and 1.5 also well cover the error caused by time discretization as in the previous computational experiments and the  $\kappa=1$  can be used for the constant heat transfer coefficient.

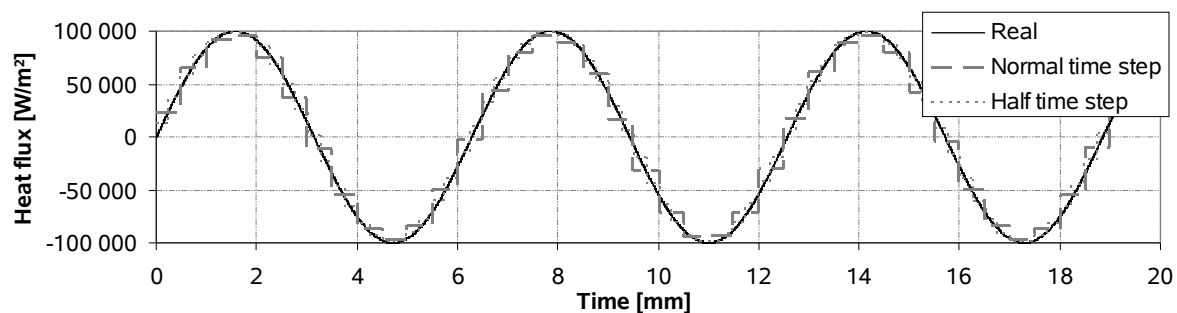


Figure 10 – Time dependent heat flux  $q = 100\,000 \cdot \sin(t)$ .

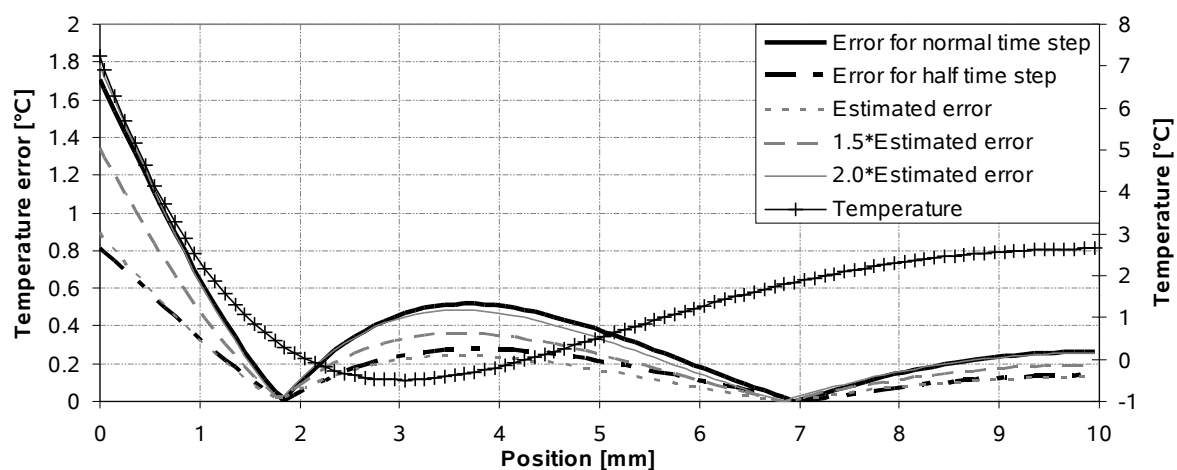


Figure 11 – Temperature profile for heat flux  $q = 100\,000 \cdot \sin(t)$  after 20 s.

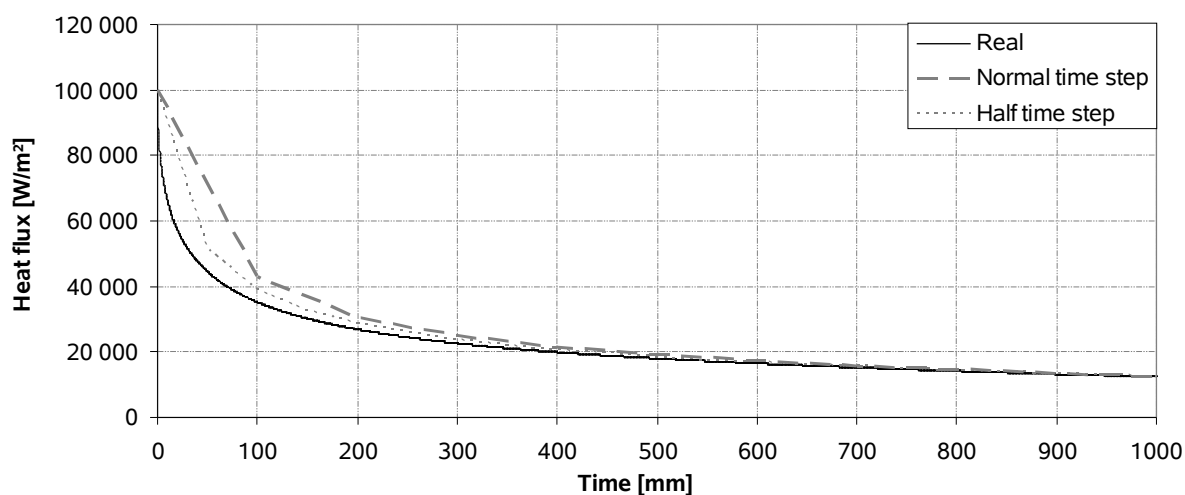


Figure 12 – Heat flux for constant heat transfer coefficient  $h = 1000 \text{ W/m}^2 \cdot \text{K}$ .

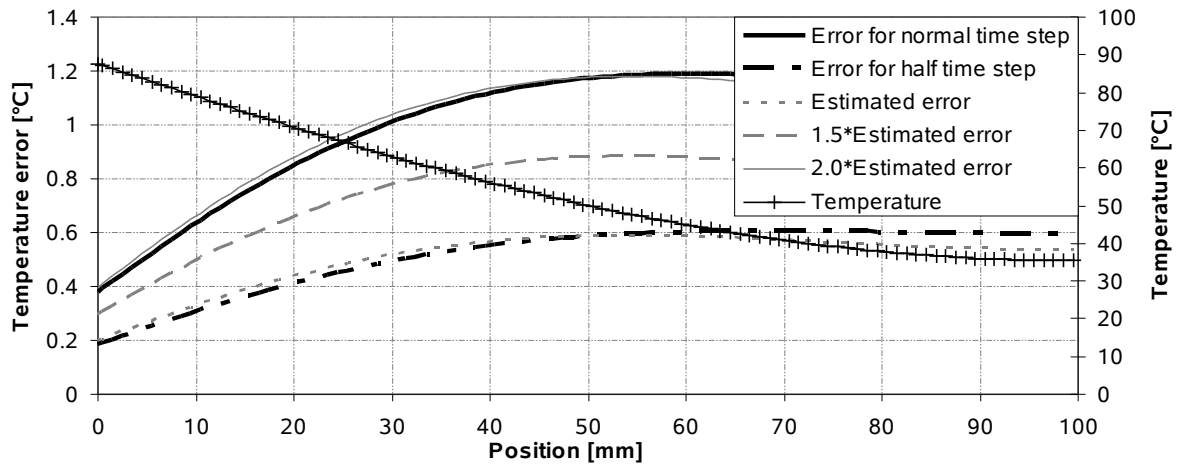


Figure 13 – Temperature profile for constant heat transfer coefficient  $h = 1000 \text{ W/m}^2\text{K}$  after 1000 s.

#### Mesh Discretization Error

Two one-dimensional models were used to verify the method for estimation of the error caused by space discretization. However, the method can also be used for multi-dimensional models. One model was assumed to be made of stainless steel and the other was a sandwich made of two pieces of stainless steel and asbestos between them. The thicknesses of steel were 30 mm and 50 mm, and the thickness of asbestos was 20mm. The starting temperature was  $0^\circ\text{C}$  and the model was exposed to a constant heat flux of  $100\,000 \text{ W/m}^2$ .

The temperature profiles were computed using a very fine mesh (20000 nodes) and a tested rough one with 20 nodes. The computed results are shown in Figures 14–16. The temperature profile computed using 20 nodes was compared with the results computed using a very fine mesh. The differences are marked as a *real error* in the figures. Next, mesh discretization error estimation was computed using Eq. (10) for the rough mesh. These values are marked as *max. estimated error*. The real errors are lower than the estimated maximum values except for very small errors in heterogeneous material and a long time step of 1000 s as can be seen in Figure 16. Also the magnitude of the real errors is comparable with the estimated maximum values.

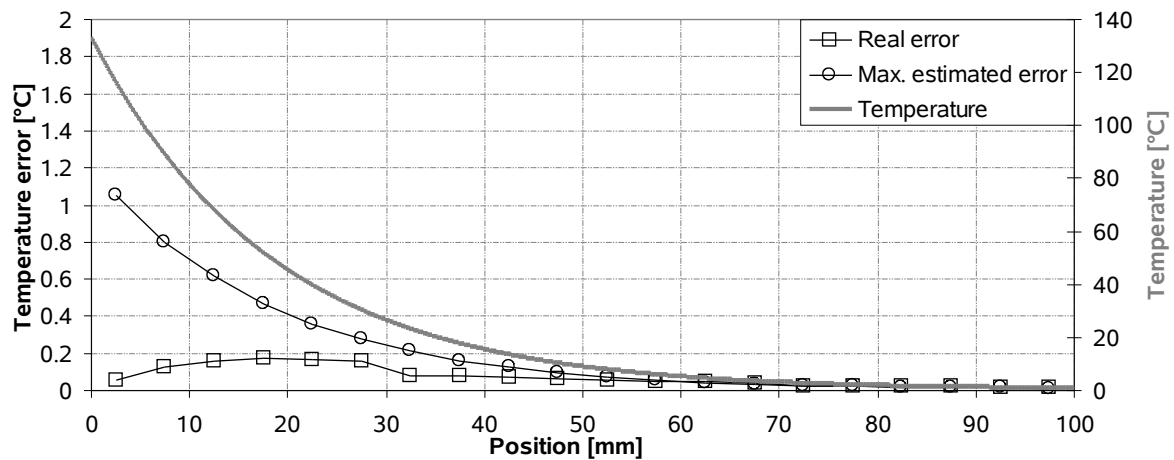


Figure 14 – Homogeneous model of steel after 100 s.

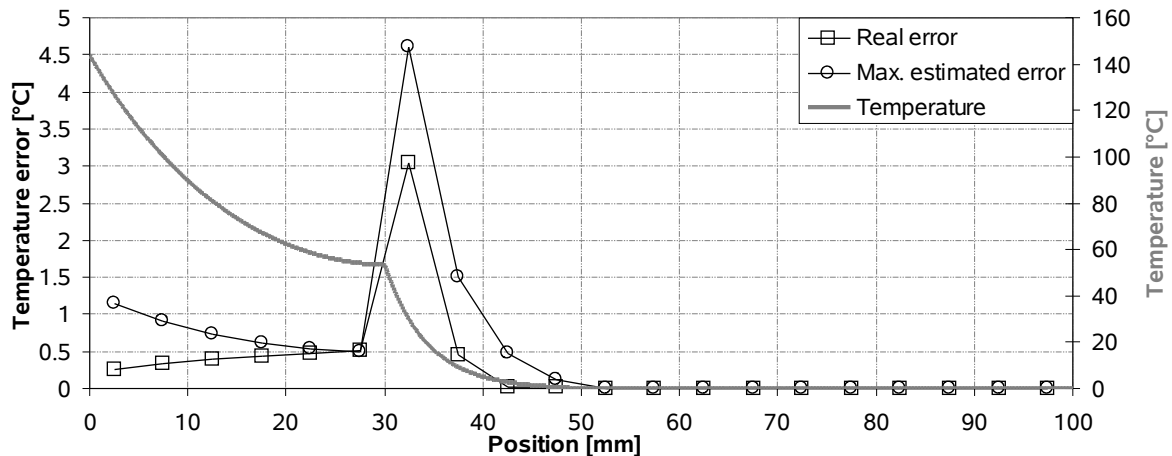


Figure 15 – Model of steel and asbestos after 100 s.

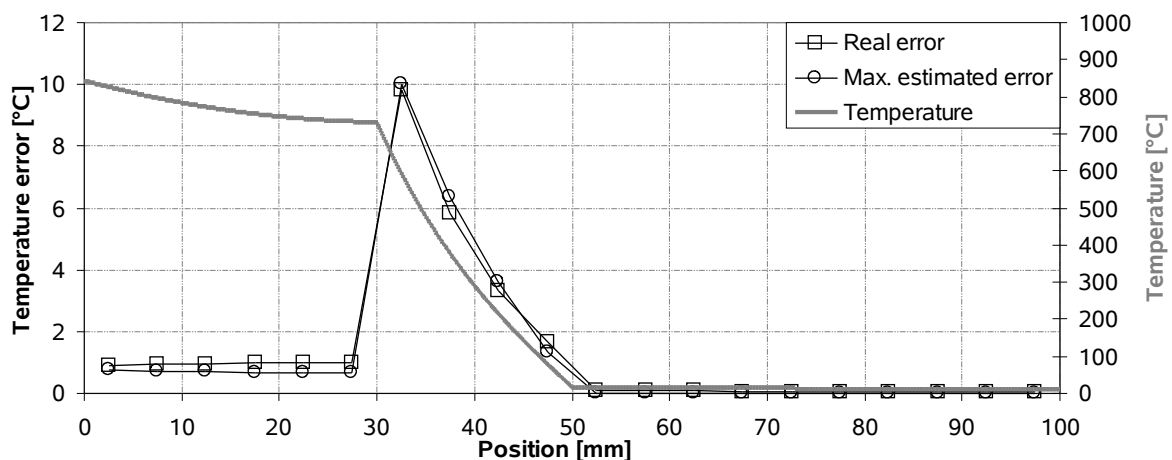


Figure 16 – Model of steel and asbestos after 1000 s.

## 5. Conclusion

The self-adaptive design of computational models and knowledge of accuracy of computed results using a numerical method are necessary. This technology makes it possible for engineers and scientists to construct more realistic mathematical models of physical processes.

The computational experiments have shown that Eq. (12) can be used for estimation of the error caused by time discretization. The only places where the equation should not be used are those where the error is very small in comparison to the maximum one. Eq. (10) should be used for the adaptive meshing to keep the accuracy of the computational model at a reasonable level. This is mainly important for multi-dimensional models where the number of nodes rapidly increases and the computation time is much longer.

## 6. Literature

- Incropera, F. P.; DeWitt, D. P. (1996) *Fundamentals of Heat and Mass Transfer*. 4th ed. New York: Wiley. ISBN 0-471-30460-3.
- Patankar, S. V. (1980) *Numerical Heat Transfer and Fluid Flow*. Hemisphere Publishing Corporation. ISBN 0-891-16522-3.
- Pohanka, M.; Woodbury, K. A. (October 2003) A Downhill Simplex method for computation of interfacial heat transfer coefficients in alloy casting. *Inverse problems in engineering*, Vol. 11, No. 5, pp. 409–424.